



**MUON SHIELDING:
DESIGN STUDIES OF HOMOGENEOUS SOIL SHIELDS AT 200 GeV**

D. Theriot and M. Awschalom

May 14, 1970

The explicit problem considered is the "shape" of a homogeneous soil muon backstop for a stopping 200-GeV proton beam. When the high-energy protons interact with the target, a large number of high-energy pions are produced. Some of these pions decay into high-energy muons. In order to reduce the muon flux to tolerable levels, a massive shield is required. The muon flux is then reduced by ranging out muons, solid-angle considerations, and scattering.

Muon-transport programs have been made available to NAL¹ which allow us to calculate the shape of homogeneous shields. This report gives the results of some studies made on the design of homogeneous soil shields.

The basic soil shield calculations were made with the following assumptions:

1. A cylindrical decay space in the target box 600 cm in length and 30 cm in diameter,
2. Pion production using the Trilling formula² with parameters to fit p-Pb π -production,
3. Multiple Coulomb scattering with energy loss after Eyges,³



4. dE/dx including the Sternheimer⁴ correction for density effect for collision losses, bremsstrahlung,⁵ pair production, and nuclear interactions,⁶

5. Soil density is 2.0 g/cm^{-3} .

The isoflux curves for these calculations are shown in Fig. 1. These curves had been reported previously in TM-204.

In order to understand the factors affecting the dimensions of the shield, some studies were made on the effects of target-box geometry, production angle, and target material, as well as dE/dx .

The first study made was on the effect of the decay-space geometry at the target. The results are shown in Fig. 2. The solid line is the 10^{-13} isoflux curve from the canonical calculation shown in Fig. 1, namely, a decay space 30 cm in diameter and 600-cm long. Such a target box could contain beams for production angles up to 25 mrad, and it would require a shield of 935 ft (285 m) overall length and a maximum radius of 17 ft (5.2 m).

If the diameter of the decay space is increased to ∞ , the shielding becomes a wall at 600 cm. The resulting isoflux curve shows an increase in radius at small depths in the shielding. This is to be expected because now the pions produced at angles greater than 25 mrad have a longer decay path.

If the diameter of the decay space is decreased to 5 cm, pions produced at angles larger than 4 mrad now have shorter decay paths.

The isoflux curve resulting is labeled "600 cm \times 5-cm target box" and while the length remains the same, the maximum radius decreases to 14.3 ft (4.35 m).

The next variation on the decay-space geometry study was to have no "true" decay space. In the previous calculations, the pion was assumed to be absorbed immediately upon encountering the shield. Now, that assumption is no longer valid since the pions are produced in the shield itself. Instead, we assume that the pion travels 1.8 interaction lengths⁷ before it is absorbed. For iron, this decay space is a hemisphere 30 cm in radius. This isoflux curve is labeled "no decay space." Its length is 837 ft (255 m) with a somewhat smaller radius than the other geometries.

The most striking results of these studies of the geometry of the shielding in the target region is the relative insensitivity of the bulk of the shield to rather dramatic changes in target geometry.

In Fig. 3 we return to the canonical 600 cm \times 30-cm target box, 10^{-13} isoflux curve. To calculate this curve, it is necessary to calculate two separate components, one corresponding to a wall-like geometry with a maximum production angle of 25 mrad, and the other corresponding to a tunnel-like geometry for all those pions created at greater angles. These two components are shown explicitly in Fig. 3. Note that there is a large overlap due to multiple Coulomb scattering. The central $\theta < 0.025$ contribution scatters far outside the 25-mrad line; similarly, the $\theta > 0.025$ contribution does not fall to zero at $\theta = 0$.

The next parameter varied was the target material. The canonical curves are for Pb targets, representative of high-Z targets. In Fig. 4 we see the 10^{-13} isoflux for a Be target compared with the canonical Pb target. These isoflux curves are normalized to one interacting proton. On the average, the pion spectrum produced from a Be target is harder than that from a Pb target. These higher-energy pions lead to harder muons, which require correspondingly larger shields to absorb them. At 200-m depth into the soil shield, there is on the average a factor of 1.6 ± 0.1 more muons $\text{cm}^{-2} (\text{interacting proton})^{-1}$ for a Be target than for a Pb target. At 250-m depth, the factor is still 1.6 ± 0.1 .

In the last study, the value of dE/dx used to calculate the muon range was changed. In our canonical calculations, the average dE/dx was calculated summing the contributions from collision losses, bremsstrahlung, pair production, and nuclear interactions. Large fluctuations are possible in the bremsstrahlung, pair production, and nuclear losses and hence large range straggling. Since the programs neglect range straggling, it was interesting to study a shield design using $(dE/dx)_{\text{coll}}$ alone. The ranges thus defined would have less straggling and smaller uncertainties. The results are shown in Fig. 5. The shield length increased from 935 ft (285 m) to 1000 ft (305 m). The radius also increased slightly at large depths. At 200-m depth, there were 1.6 ± 0.2 more muons $\text{cm}^{-2} (\text{interacting proton})^{-1}$ than in the canonical case of dE/dx total. At 250 m-depth, the factor increased to 2.2 ± 0.2 .

Figure 6 shows a collection of isoflux curves for the $600 \text{ cm} \times 30 \text{ cm}$ target box geometry with Pb target calculated using dE/dx from collision losses alone. These may be more appropriate to use in designing muon shielding than those of Fig. 1 where dE/dx from all contributions was used.

At this time, we have not performed calculations using pion production models other than Trilling's. However, a few general statements may be made about the differences to be expected. In the pion-energy region of 60 to 180 GeV, the CKP, Haegedorn-Ranft, and Trilling models agree within a factor of two. At the extreme high-energy end, the models have greater differences, but since the total production in this region is relatively small, the differences should not affect the shielding requirements significantly.

Therefore, one would expect that pion-model effects would produce shifts in the isoflux curves equivalent to factors of about two or less.

Conclusions

To use the given curves (Figs. 1 and 6) for muon backstop estimates, several factors must be taken into consideration before applying the flux-to-dose conversion factor,

uncertainty in production model	2
Be to Pb flux ratios	1.6
range straggling, if using Fig. 1	2 ± 0.2 .

To convert from flux to dose rate, the conversion factor is $7.8 \mu\text{cm}^{-2} \text{sec}^{-1}$ for 1 mrem/hr.

Hence, if one wants to use the canonical set of isoflux curves (Fig. 1) to calculate dose rates per interacting proton in the canonical target box, one should multiply the given curves by $2 \times 2 \times 1.6/7.8 = 0.82$.

Thus, an isoflux curve of 10^{-13} and an incident proton current of 1.5×10^{13} p/sec ($\approx 1 \times 10^{13}$ effective proton interaction), corresponds to a dose rate of 0.82 mrem/hr.

It must be warned that these calculations have been exercises in the design of ideal muon backstops without voids for beam pipes, beam-transport magnets, personnel access tunnels for magnet maintenance, etc. Estimates of real shield configurations can only be made with the aid of Monte Carlo analog calculations. These will be reported at a later time.

Acknowledgment

We want to thank Dr. R. G. Alsmiller and Mr. J. Barish of Oak Ridge National Laboratory for supplying the computer programs used in these calculations as well as for modifying them to suit geometries different from those of the original programs.

REFERENCES

- ¹R. G. Alsmiller, Jr., M. Leimdorfer, and J. Barish, High Energy Muon Transport and the Muon Backstop for a 200 GeV Proton Accelerator, Oak Ridge National Laboratory Report ORNL-4322, Nov. 1968.
- ²J. Ranft and T. Borak, Improved Nucleon-Meson Cascade Calculations, National Accelerator Laboratory FN-193, Nov. 1969, p. 9.
- ³L. Eyges, Phys. Rev. 74, 1534 (1948).
- ⁴R. M. Sternheimer, Phys. Rev. 88, 851 (1952); Phys. Rev. 103, 511 (1956); Phys. Rev. 115, 137 (1959); Phys. Rev. 124, 2051 (1961); Phys. Rev. 145, 245 (1966); and Phys. Rev. 164, 349 (1967).
- ⁵P. J. Hayman, N. S. Palmer, and A. W. Wolfendale, Proc. Roy. Soc. A275, 391 (1963).
- ⁶P. M. Joseph, Nucl. Instr. and Methods 75, 13 (1969).
- ⁷D. Keefe and C. M. Noble, Radiation Shielding for High Energy Muons: The Case of a Cylindrically Symmetrical Shield and No Magnetic Fields, Lawrence Radiation Laboratory Report UCRL-48117, March 1968.

Figure 1:

Canonical Muon Shields
Isoflux Curves (Muon cm^{-2}
(interacting proton) $^{-1}$)
Shielding Material: Soil
Target Material: Pb
Target Box Geometry: 600 cm x 30 cm
(dE/dx)_{tot} used to calculate ranges.

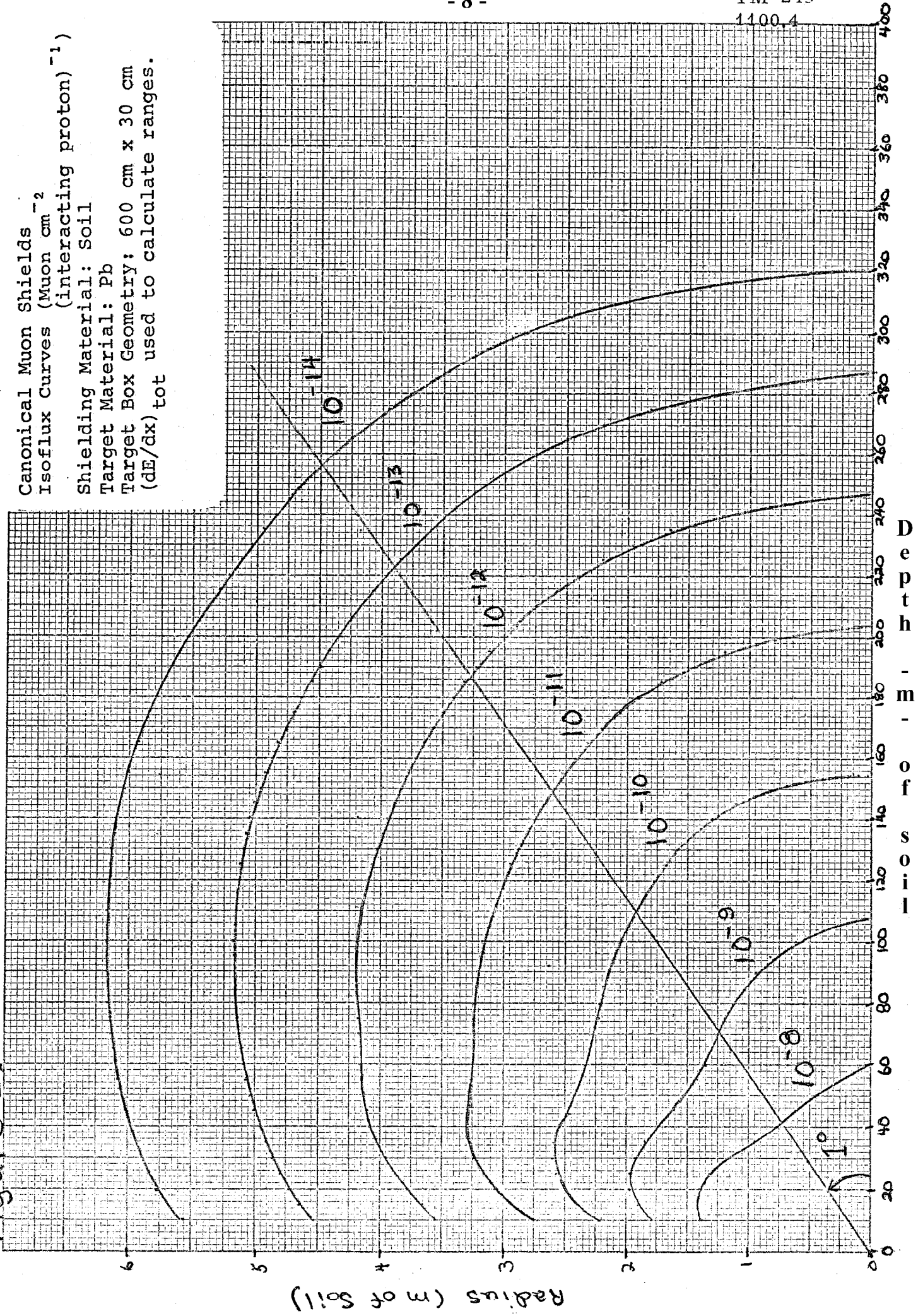
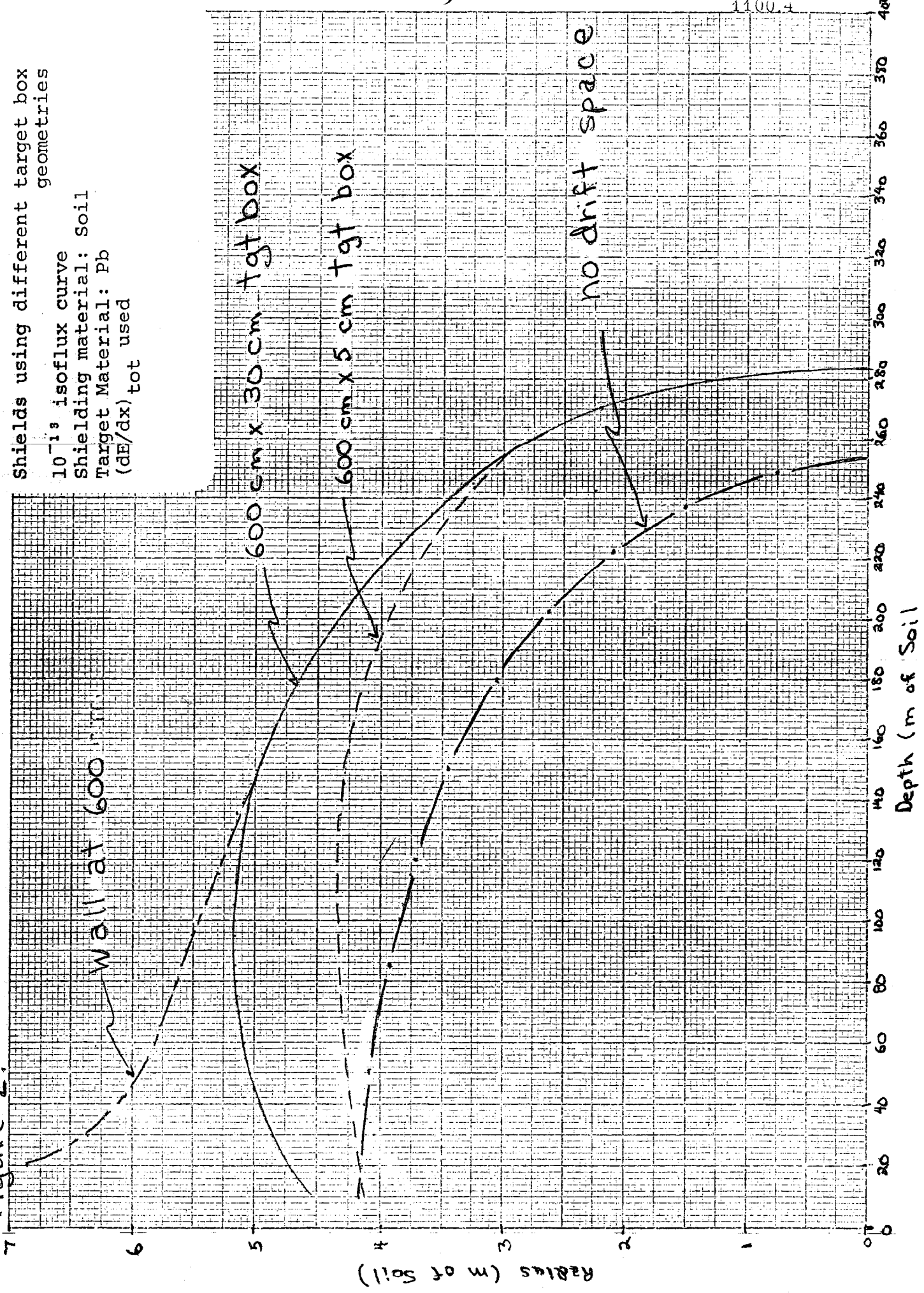


Figure 2:

Shields using different target box geometries
 10^{-13} isoflux curve
Shielding material: Soil
Target Material: Pb
(dE/dx)_{tot} used



Two angular contributions to shield
 10^{-13} isoflux curve
 Shielding Material: Soil
 Target Material: Pb
 Target Box Geometry: 600 cm x 30 cm
 $(dE/dx)_{tot}$ used

Figure 3:

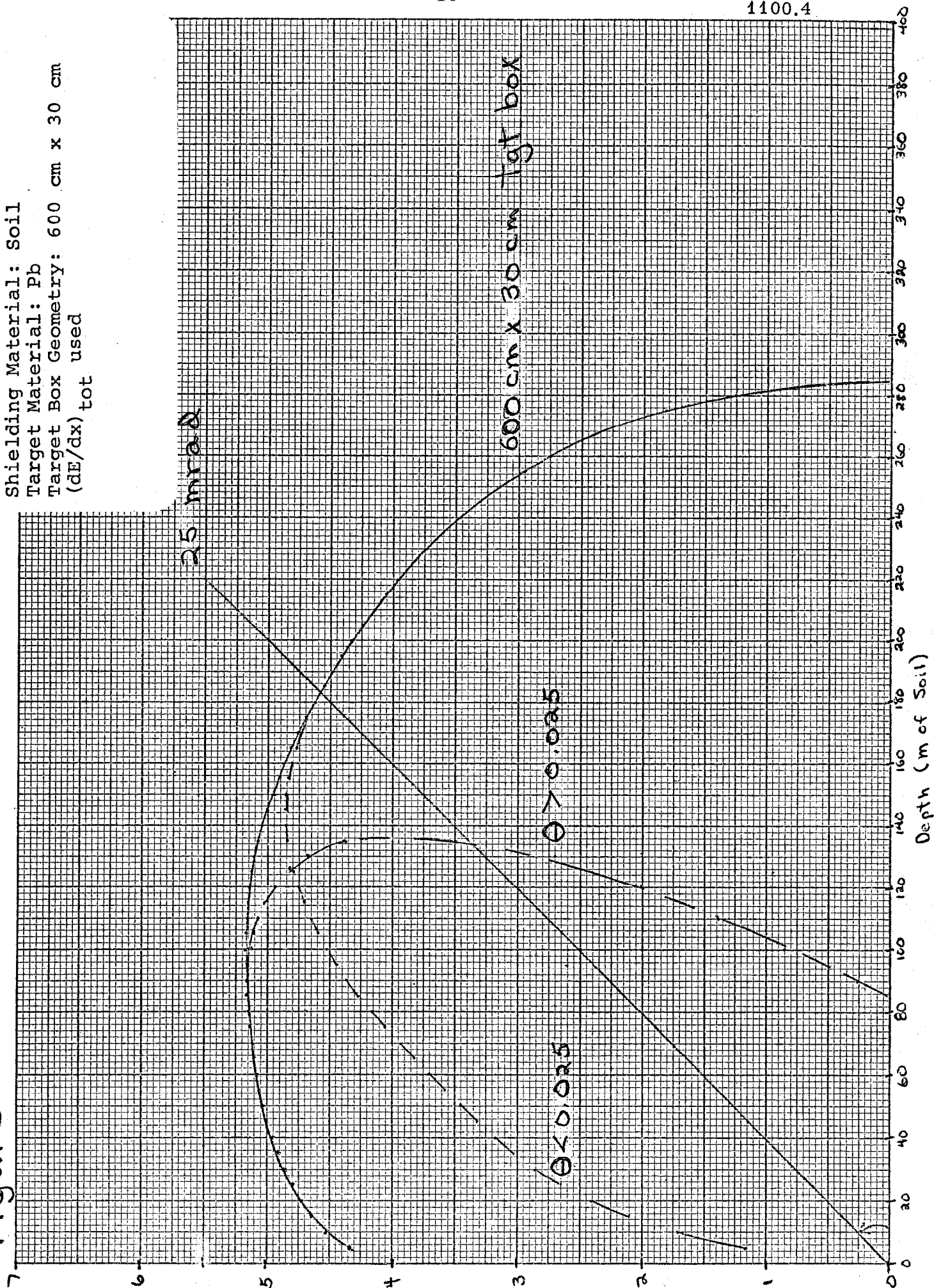


Figure 4:

Shield using Be target versus Pb target
 10^{13} isoflux curve
 Shielding Material: Soil
 Target Box Geometry: 600 cm x 30 cm
 $(dE/dx)_{tot}$ used

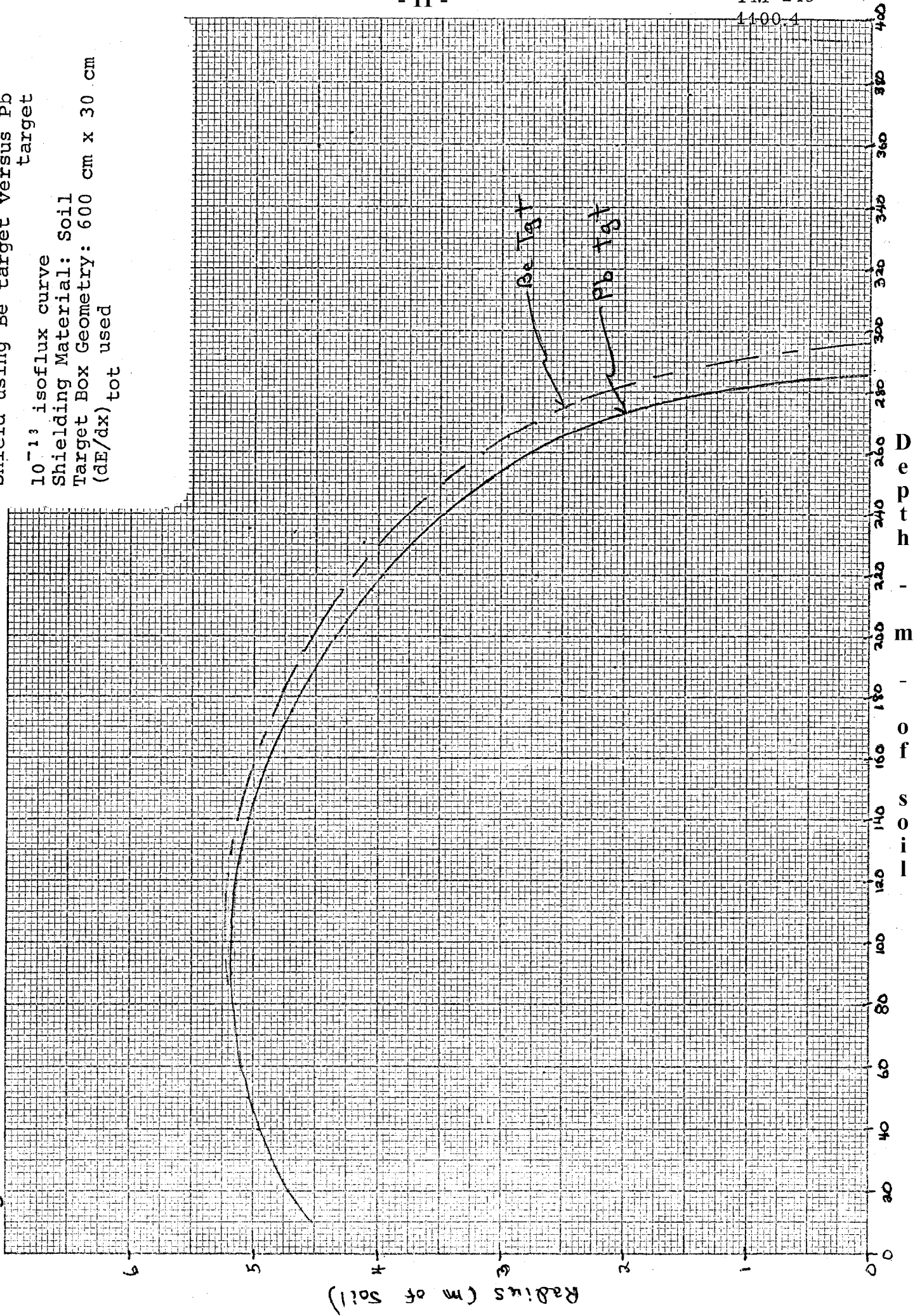


Figure 5:

Shield using $(dE/dx)_{coll}$ versus
 $(dE/dx)_{tot}$
 10^{-13} isoflux curve
Shielding Material: Soil
Target Material: Pb
Target Box Geometry: 600 cm x 30 cm

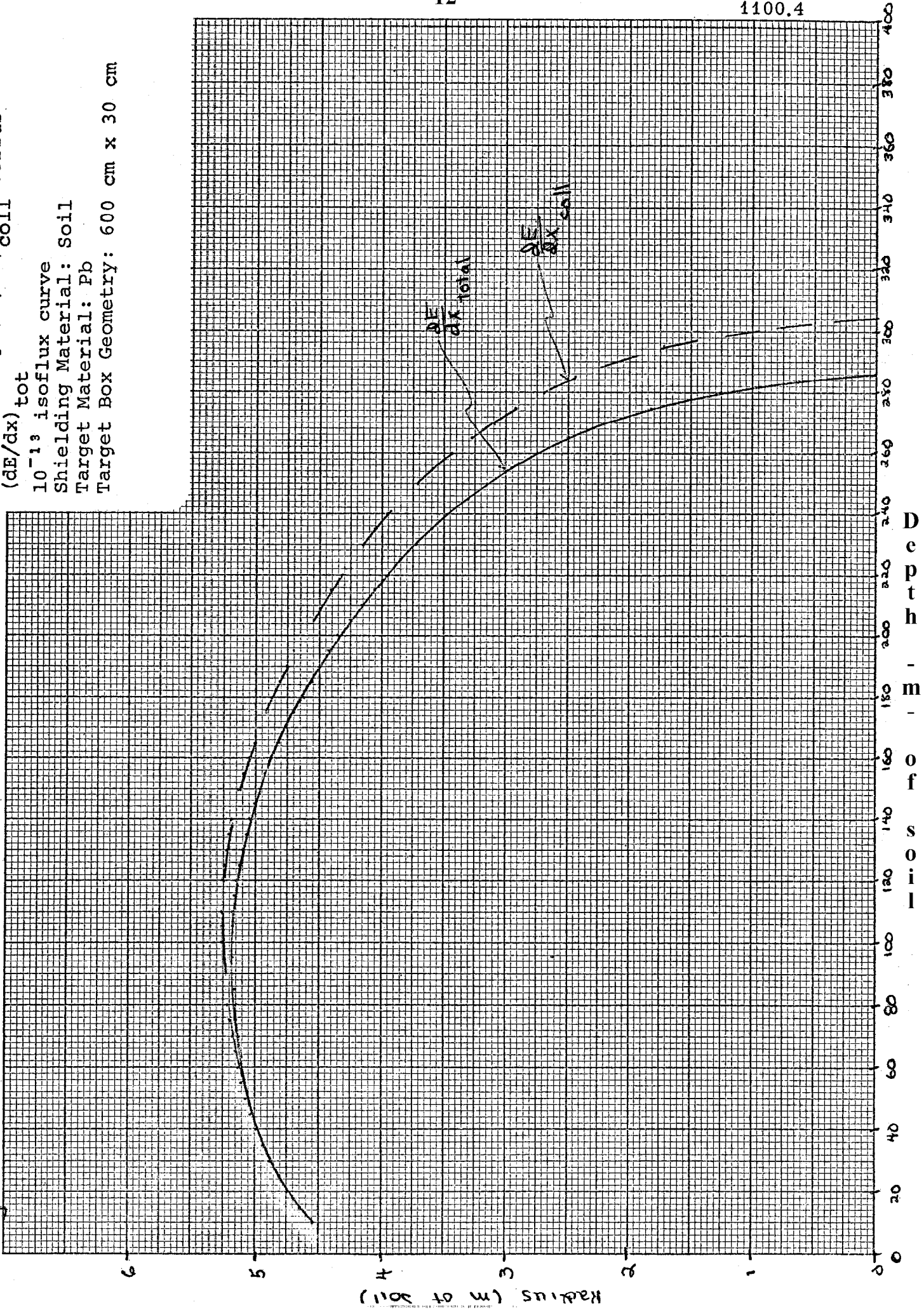


Figure 6:

Muon shields using $(dE/dx)_{coll}$
 IsoFlux curves ($\mu\text{on cm}^{-2}$
 (interacting proton) $^{-1}$)
 Shielding Material: Soil
 Target Material: Pb
 Target Box Geometry: 600 cm x 30 cm

